Ethanol/Water Separation by Linda Type A Membrane

Zhuoqi Zheng
Qingdao Agricultural University https://orcid.org/0000-0003-3758-2756
Yan Li (1310757678@qq.com)
Qingdao Agricultural University

Research Article

Keywords: LTA molecular membrane, Membrane filtration loss, ethanol concentration

Posted Date: November 1st, 2021

DOI: https://doi.org/10.21203/rs.3.rs-964893/v1

Abstract

Ethanol / Water Separation Technology is a long term research. LTA molecular sieve, which is an industrially important desiccant as a kind of zeolite molecular sieve. It is always used in the reverse osmosis method, which is one of the sea water desalination, and extraction of industrial ethanol method in the world. Membrane separation technology is widely used in cell science[1, 2], human science[1, 2], microbial science[3], military industry, battery technology[4, 5] and so on. With 2 years invention and attempts, prototype membrane is finished and the filtered data has also been measured in different side, such as Linda Type A(LTA) making temperature, raw material ratio of membrane preparation and filter curves. The physicochemical analysis of the samples before and after filtration was carried out. The manbrane filtration losses are very low and can be used with food grade filtration

1. Introduction

LTA molecular sieve, which is an industrially important desiccant as a kind of zeolite molecular sieve. Membrane separation was first used in cytology[6] and is now widely known as its application in seawater desalination[7, 8]. The field of biotechnology is developing rapidly, but 4A molecular sieves is rarely used in food. The design and experiment are based on food-grade applications, and the food-grade filtration membrane was synthesized innovatively, then the loss of membrane filtration was also analyzed.

Membrane separation technology

The technology of membrane separation apply to different pressure and different concentration, then separate substances as potential differences[9, 10]. That is to say, molecular sieving and selective adsorption[11] and separation molecular sieving[12] mainly apply to the voids in the membrane layer to sieving substances to achieve separation. The difference in particle size of the material is used to select a membrane material with a suitable pore structure with a particle size larger than the pore size. Substances smaller than the membrane pore size pass through the membrane to the other side under the driving force. According to different retention, it is divided into surface retention and internal retention[13].

Now, there are several methods for alcohol free beer or low alcohol beer production. physical methods such as vacuum distillation[14], Reverse Osmosis[15, 16] and Osmotic Distillation[17]. Membrane-based processes include Reverse Osmosis, Nanofiltration[18–20], Dialysis and Pervaporation[21]. And the vacuum evaporation is the cheapest and the most common process[22].And in wine industry, Electrodialysis[23, 24], Reverse Osmosis, Membrane Contactor are frequently used, but the cross-flow microfiltration(CFMF)[25–27] are widely put into use. However, in the development of CFMF membrane filtration, wine has long been affected by membrane contamination. The main consequences of this pollution are poor film performance, high cost, and excessive residue of some wine components, which may lead to the loss of certain sensory properties[28–30]

This design adopts LTA molecular sieve (4A molecular sieve). The LTA molecular sieve membrane has been confirmed due to excellent performance in ethanol / water separation, and can be used under higher working temperature and organic solvent conditions[31–33]. Zeolite membranes are widely used in the field of separation due to their excellent thermal, chemical stability, regular pore structure, and marvellous selectivity of adsorption. Zeolite membranes applied in the food industry will not face the above-mentioned problems. Pure silica zeolite membranes (Silicalite-1 and Silicalite-2)[34] have strong hydrophobicity because they do not contain aluminum in the skeleton, and they have preferential adsorption properties for ethanol, so they can be used in fermentation to produce ethanol-permeable processes.

2. Materials And Methods

2.1. Materials

The main reagents used in this experiment is to make LTA membrane. Sodium metaaluminate ($NaAlO_2$), sodium hydroxide (NaOH), deionized water, sodium silicate. Nonahydrate ($NaSiO_3.9H_2O$) is prepared for LTA membrane.

The main sample liquor is alcohol solution and red wine.

2.2. Preparation of LTA powder

LTA molecular sieve membrane is widely used in industry to selectively remove water from organic matter by pervaporation[35]. For LTA molecular sieves, the maximum dynamic diameter of molecules capable of diffusing in their channels is 0.42 nm. The ethanol molecular dynamics ranges from 0.47 to 0.51 nm, and the water molecular dynamics begin from 0.27 nm, then until to 0.32 nm. Therefore, ethanol molecules cannot pass through the pores because of the dynamic diameter larger than the pore size of LTA, but water molecules However, because of its small dynamic diameter, it can pass smoothly, thus realizing "molecular sieve"[36, 37].

The method is that the LTA seed is synthesized by hydrothermal method. The material ratio of the seed liquid is n (Na_2O): n (Al_2O_3): n (SiO_2): n (H_2O) = 3.5: 1: 2: 125. The concrete synthetic measures: dissolve 8.00g NaOH in 18mL H_2O, add 9.36 g $NaAlO_2$ and stir until clear[38, 39]. Slowly add 13.73 g silica sol under vigorous stirring conditions, and stir at 25℃ for 1 h to mix the reactants 5 h. After homogenization, transferred into a 50 mL stainless steel reactor with a polytetrafluoroethylene lining, and allowed to stand at 100℃ for 1.5 hours. The final product was dried at 60℃ after washing three times with deionized water.

Preparation of LTA molecular sieve membrane: The LTA molecular sieve membrane is prepared by the secondary growth method, and the reaction solution is according to the preparation method of the LTA seed solution and n (Na_2O): n (Al_2O_3): n (SiO_2): n (H_2O) = 2: 1 : 2: 135. Specific steps: Place the pre-coated ceramics vertically in the reaction kettle, pour the reaction solution, and crystallize at 100℃ for 5

h. After the completion of the crystal, the reaction kettle was taken out, and it was rapidly cooled with tap water. The molecular sieve membrane was dried at 60℃ after that it washed with deionized water and soaked in deionized water for about 15 hours. The molecular sieve membrane preparation process is shown in Figure 3.

2.4. LTA membrane separation performance test of ethanol / water mixed solution

The process of alcohol / water separation is carried out under normal temperature, and the separation device is shown in Figure 10. The osmotic vapor-liquid separation test device is mainly composed of the following parts: ① solution to be separated; ② peristaltic pump; ③ separation mold; ④ condenser; ⑤ vacuum pump; ⑥ liquid chromatography. Put the prepared LTA membrane into the mold for sealing, connect the peristaltic pump at one end to inject the solution to be separated into the mold to make it contact with the membrane, and the solution that does not penetrate the membrane will continue to circulate back to the container containing the solution; at the other end, decompress the system through the vacuum pump, vaporize the solution through the membrane and collect it through the condensation device, and finally send it to the chromatography for component analysis. The permeate flow of LTA membrane (P_i : $kg{\cdot}m^{-2}{\cdot}h^{-1}$) is calculated by formula (1).

$$\mathrm{Pi} = \frac{Mi}{A \times t}$$

In the Formula, M_i is the mass of the permeate (unit: kg), A is the effective area of the membrane (unit: m^2), and t is the time of the separation process (unit: h). The selectivity of LTA membrane is evaluated by calculating the separation factor ($\alpha_{I, J}$), which is calculated according to formula (2)

$$\alpha\mathrm{i,j} = \frac{Xi/Xj}{Yi/Yj}$$

2.5. Design and production of filtration equipment

There are 52 kinds of aroma components of sample (Cabernet Sauvignon) in dry red wines.[40] These substances are measured by Solid Phase Microextraction (SPME)[41, 42] The molecular weight or molecular diameter of all these aroma components are larger than the maximum kinetic diameter of the molecules diffusing in the pore channel of LTA molecular sieve membrane (4A molecular sieve) by 0.42nm.Therefore, the wine is filtered through the pore of LTA molecular sieve membrane (4A molecular sieve), and the water is filtered out to retain alcohol and aromatic components. Weigh the volume of filtered water, calculate the percentage of residual alcohol in the original volume, i.e. the volume fraction of existing solution alcohol, and conduct many times parallel experiments.

2.6 Reversed phase high performance liquid chromatography(RP-HPLC)measuring organic acid change

The wine sample was diluted 10 times with ultra pure water and filtered by 0.22 μm water microfiltration membrane. The filtrate was to be tested

Chromatographic column: diamonsil C_{18} (4.6 mm × 250 mm, 5 μm); mobile phase A: 7% methanol, B: 0.01 mol / Na_2P0_4 buffer (pH = 2.2); gradient elution: 1 min, 25% A, 0.01~4 min, 60% A, 4.01~7.0 min, 80% A, 7.01~12.0 min, 80A; flow rate: 0.6 mL/ min; column temperature: 25 ℃; injection volume: 20 μL; detection wavelength: 210nm.With 11 organic acids as variables and wine samples as test objects, principal component analysis was carried out by SPSS statistics.[43–45]

2.7 Determination of 20 amino acids in wine sample by Reversed Phase High Performance Liquid Chromatography

The amino acids are derived into compounds which are good for separation and detection. DNFB pre column derivatization is used to make amino acids absorbed at 360nm. At the same time, the combination of DNFB and gradient elution program can be used for qualitative and quantitative detection. The wine samples were centrifuged by freezing (12000r / min, 15min, 4 ℃), the supernatant was taken, filtered by 0.45 μm water phase membrane and analyzed.[46, 47]

2.8 Comparison of antioxidant activity by Iron reduction capacity experiment

Take 0.35 ml of 1, 0.5, 0.25, 0.125, 0.0625, 0.03125 wine samples of different dilution concentrations, add PBS (625ml 0.2mol·mL^{-1} $Na_2H_2P0_4$ and 375ml 0.2mol NaH_2P0_4, pH = 6.6) and 1% potassium ferricyanide (K_3[Fe (CN) $_6$]) into the corresponding volume, and cool to 25℃ in water bath at 50℃for 20min, then add 0.35ml 10% Trichloroacetic acid was centrifuged at 3000rpm for 10min, 1.2ml of supernatant was taken, 1.2 ml of distilled water and 0.24ml of 0.1% $FeCl_3$ were added respectively, and the OD was measured at 700nm. Trolox was used as positive control. In the negative control, water is used instead, and the rest is the same as the sample to be tested.[48]

2.9 Filtrate alcohol data accuracy detection

Distill with Italian machine Stillatore Elettronice Enochimico (DEE) distiller, carry out sampling inspection, and check and verify the alcohol accuracy with the method of measuring alcohol accuracy with specific gravity alcohol meter.

3. Results And Discussion

3.1 Characteristics of LTA membrane

LTA molecular sieve $|Na_{12}{}^{+}(H_2O)_{27}|\cdot[Al_{12}Si_{12}O_{48}]_8$ has a three-dimensional eight-membered ring vertical channel structure in Figure 4. It can be obtained from the XRD spectrum [Figure. 5 (a)] that the spectrum of LTA molecular sieve seed is in good agreement with the standard spectrum, and there is no impurity

peak. It is proved that the seed is a pure phase of LTA molecular sieve. By controlling the synthesis conditions, LTA molecular sieve crystal with uniform size is obtained as the seed for preparing membrane materials. Follow the SEM picture [Figure. 5 (b)], it can be seen that the crystal is in cube shape with uniform size, the diameter is 0.5-1 μm.

Scanning Electron Microscope (SEM) photos of LTA powder and LTA membrane are shown in Figure 6. From Figure. 6 (a), it can be seen that the LTA powder crystal has a cubic shape with a size of 1-2μm and a relatively uniform size distribution. It can be seen from Figure. 6 (b) that the thickness of LTA membrane is small (about 5μm), which is the key to obtain high permeability flow. High permeability flow can ensure that the separation process can be completed in a short time in industrial application, and it is a standard to measure the quality of membrane. It can also be seen from the front photos of LTA membrane that the membrane is continuous in large area, completely covered on the surface of the carrier, the crystals in the membrane are completely mutual generated, and there are no defects visible to the naked eye [Figure. 6 (c) and (d)], which is the decisive factor to achieve high selectivity, while high selectivity is the guarantee of high purity of industrial products, and it is also the first assessment Another important standard for the quality of a membrane.

The X-ray Diffractometer (XRD) spectrum of LTA powder and LTA membrane is shown in Figure 7, which is in good agreement with the characteristic peaks in the simulated LTA spectrum, and there are no other characteristic peaks except for the carrier tube. It is further confirmed that the synthesized LTA powder and LTA membrane are pure phase. At the same time, the high intensity of the diffraction peak indicates that the crystals in the powder and the membrane have good crystallinity and the pore structure is complete.

The surface of the support α - Al_2O_3 ceramic tube is rough and porous, and the pore size is 3-7 μ m [Figure. 8 (A)]. The seed coating prepared by dip coating method has the smallest coverage ratio, some of the pores are not filled, and there are a large number of exposed Al_2O_3 particles [Figure. 8 (B)]. Literature[49, 50] also reported that this method has a low membrane formation rate and needs many hydrothermal synthesis. The seed liquid scraping method is used. The covering effect of seed preparation layer is better than that of dip coating method, but there are still Al_2O_3 particles exposed [Figure. 8 (C)], which may be due to the low viscosity of seed liquid, the seed is very loose on the surface of the body, and easy to fall off. In order to enhance the adhesion between the seed and carrier of molecular sieve, and prevent the crystal from falling off during synthesis, the seed preparation layer is prepared by seed slurry scraping method[51]. It can be obtained from Figure. 8 (D) The seed layer is completely and relatively dense on the surface of ceramic tube without exposed area. In the course of hydrothermal synthesis, the synthetic liquid as a binder is expected to be transformed into molecular sieve crystal, or provide the materials needed for the formation of molecular sieve membrane, which may not bring additional resistance to the molecular sieve membrane. Molecular sieve synthetic liquid as a binder has certain universality[52, 53].

In Figure 9, the molecular sieve membrane synthesized by the combination of scraping crystal seed slurry and secondary growth method is relatively compact and flat, with a membrane thickness of about 20 μm in Figure. 9(B)

3.1 Separation performance test of alcohol / water

The results of the alcohol / water separation performance test of the LTA membrane are shown in Figure 11. As can be seen from Figure 11 (a) and Figure 11 (b), the permeation flow rate of ethanol is generally low, and it shows an increasing trend with the increase of the mole fraction of ethanol in the injection solution. The flow rate gradually increases with increasing temperature. The penetration rate of water at different temperatures is much higher than that of ethanol, but the change trend is the same. Because the dynamic diameter of water molecules is smaller than that of ethanol molecules, it is easier to diffuse into the pores of the membrane, so the infiltration flow rate of water is significantly higher than that of ethanol. As the temperature increases, the thermal motion of the molecules increases, and the number of molecules permeating the membrane, whether water or ethanol, will increase, leading to an increase in osmotic flow. As the concentration of ethanol in the injection solution increases, the chance of ethanol molecules entering the pores of the membrane increases, and at the same time, the passage of water molecules is also inhibited. Therefore, the infiltration flow of ethanol shows an increasing trend, but water is the opposite.

According to formula (2), the separation factor corresponding to different temperature conditions and different ethanol concentrations in the injection solution can be calculated from the permeation flow data. The results are shown in Figure 11 (c). It can be seen that the separation factor increases with the increase of the test temperature, but under the 9 test temperature conditions, the best separation effect is obtained when the ethanol mole fraction is 60%. When the ethanol concentration continues to increase, the separation efficiency has Significantly reduced. In order to consider the stability of the LTA membrane, a long-term continuous work test is required. See Figure 11 (d) for the curve of the total permeation flow rate and separation factor of the membrane as a function of time when the alcohol: water = 1: 1 (substance amount ratio) in the injection solution at 25℃. The total permeation flow rate of the LTA membrane fluctuates around 6kg·m^{-2}·h^{-1}, and the separation factor is basically stable at about 5,500, which shows that the LTA membrane has very good thermal and mechanical stability and can be cycled many times. It can be used repeatedly for many times, which is beneficial to industrial applications and reduces production costs.

The composition of the feed liquid directly affects the solubility of the components in the pervaporation membrane, which in turn affects the diffusion coefficient of the components in the membrane and the final separation performance., With the increase of the concentration of the preferential osmotic component in the feed liquid, the total osmotic flux and ethanol flux increase significantly while the water flux is basically unchanged, because, as the ethanol concentration increases, the contact between ethanol and the membrane surface increases As the adsorption capacity increases, the ethanol flux increases; while the water concentration changes little with the increase or decrease in ethanol concentration, the water flux remains basically unchanged. As the concentration of raw material ethanol

increases, due to the resistance of the membrane separation process, the concentration on the permeate side does not increase linearly with the increase or decrease in the concentration of raw material ethanol, resulting in the decrease in ethanol concentration with the increase in the concentration of raw material side.

3.2 Formula deduction and testing

3.2.1 Formula deduction

Alcoholic aroma molecules and volatile molecules have molecular dynamics diameters larger than those of water molecules, so only water molecules will be filtered at the other end of the filter, and alcohols and other molecules have dynamic diameters greater than those of water molecules. It will not be filtered and will remain at the end of the filter, so that the concentrated liquor will retain the original flavor and chemical composition without being damaged by high temperature or chemical concentration. After being filtered, the concentrated liquid can be obtained by weighing the quality of filtered water, evaporating and cooling to obtain the liquid remaining on the filter (LTA membrane), so as to obtain the concentrated sample.

The final product alcohol degree is expressed by formula 3

$$\beta = \frac{ma}{\frac{ma}{ma+(mb-mq)+mc} * 100\% * ma + mw}$$

β is the alcohol of the final product, ma is the mass of the liquid left after filtration, m_b is the mass of the filtration equipment after filtration, m_q is the mass of the filter equipment before filtration, m_c is the mass of the filtered liquid, mw is the quality of the distilled water added after filtration, m_z is the initial liquid mass of this confirmatory experiment, § is the alcoholic strength of the initial alcohol solution.

The control of alcohol level solves the shortcoming that the alcohol level of the product cannot be accurately measured, and makes the alcohol level make products more in line with the market within a controllable range. It can better save factory cost, save time consumption in alcohol level detection, and reduce the measurement error of alcohol level.

According to Table 5. Alcohol error less than 1%.

3.2.2 Sample composition analysis before and after

3.2.2.1 Reversed phase high performance liquid chromatography(RP-HPLC) measuring organic acid change

The organic acids in wine samples were determined respectively. Because of the differences between bottles, the types and contents of organic acids were also different.

According to Table.6, the total amount of organic acid will be reduced after filtration, but the reduction proportion is less than 10%, which can be judged as the normal loss of organic acid in the filtration

process. Both VC and fumaric acid are trace, so it is impossible to judge how much they are reduced. Tartaric acid loss is the lowest in the detection, about 2%, and the most important tartaric acid loss in wine sample is the lowest, which ensures the quality of wine samples after filtration.

Most of the filter liquid staying in the filter layer can not be recycled, which makes the loss of some nutrients in wine samples inevitable. However, the loss rate of organic acids in the filtration process is low. It can be concluded that organic acids perform well under the filtration of LTA membrane.

3.2.2.2 Determination of 20 amino acids in wine samples by Reversed Phase High Performance Liquid Chromatography

The filtration loss rate of amino acids is about 2%. It can be seen that the loss percentage of amino acids is greater than that of organic acids. However, only 2% of amino acids are lost, which has no significant impact on the taste and nutritional value of wine samples. There is no direct large-scale loss of amino acids in the table, which proves that the LTA The loss of amino acids in the process of membrane filtration is not more than expected

3.2.2.3 Comparison of antioxidant activity by Iron reduction capacity experiment

In the experiment of iron reduction ability, antioxidants give electrons through their own reduction effect to remove free radicals. The antioxidant in the sample can reduce Fe^{3+} of potassium ferricyanide (K_3[Fe (CN) $_6$]) to Fe^{2+}, and form Prussian blue (Fe_4 [Fe (CN) $_6$]$_3$,) with ferric chloride, which has the maximum absorbance at 700nm. Therefore, the antioxidant activity of potassium ferricyanide (K_3[Fe (CN) $_6$]) can be explained by measuring its reducing power. The stronger the reducing power is, the stronger the antioxidant capacity is.

The IC_{50} of red wine samples is 0.033, which means that when the absorbance value is 0.5, the dilution concentration of red wine samples is 0.033.

It can be seen from reducing power assist that the antioxidant capacity of wine samples has decreased, but the reduction ratio is not high, which belongs to normal filtration loss. It is determined that the loss of polyphenols and proteins in the filtration process results in a reduction ratio of less than 5%, which can ensure that the vast majority of antioxidant substances remain, and the antioxidant components of wine samples have a low loss in the filtration process.

4. Conclusion

The membrane separation of ethanol and water is very useful in the real society, but it has not fully played its role in the wine of food. In this experiment, the LTA film is made gradually by making the LTA powder. Finally, the alcohol filtration experiment of wine is carried out. According to many groups of data, the formula is obtained, which realizes the data-based measurement of wine precision. The error of the formula in this experiment is low, and it can be put into production. This experiment is not only limited to the deduction of formula, but also more analysis of chemical components before and after wine

separation and filtration. The change of organic acids before and after filtration was measured by reverse high performance liquid chromatography. Although the organic acids were lower than before filtration, the quantity was smaller, less than 2%, and there was no significant change in the acidity and quality of wine. The change of 20 kinds of amino acids in wine before and after filtration was determined by reverse high performance liquid chromatography. The kinds of amino acids before and after filtration did not change. Although the amount of amino acids decreased, it would not have a great impact on the stability of wine within the controllable range, and the decrease was less than 2%. The antioxidant capacity of wine was compared before and after. Although the antioxidant capacity of wine decreased, it still did not affect its nutritional value and sensory value, and the degree of reduction was less than 2%.

However, the production of LTA membrane in this experiment has greatly reduced the cost of human resources and saved time, human and financial resources. Due to the limited experimental capacity, more chemical composition analysis and comparison in wine have not been well tested, but in the known experimental results, all components of wine have declined after filtration. The filtration of this LTA membrane will reduce the total amount of all components in wine, but the proportion of reduction is not high, so this LTA membrane has the value of production.

5. Discussion

LTA molecular sieve, which is an industrially important desiccant as a kind of zeolite molecular sieve. It is also called 3A, 4A, and 5A molecular sieves according to the differences in cations and pore sizes. In other words, when the ethanol / water mixture flows through the LTA membrane, if it is collected at both ends of the membrane, in principle, pure water and ethanol-free can be obtained under low energy consumption and pollution-free conditions. This object is to realize the separation of ethanol / water by preparing LTA zeolite molecular sieve material as a membrane on the outside boundary of alumina tube. Kyohei Ueno et al.[54] have studied Hydrophobic pure-silica *BEA-type zeolite membranes by hydrothermal synthesis using a secondary growth method and were applied to the separation of alcohol/water mixtures by pervaporation (PV), which is excellent properties, high thermal stability, and unique large pore structure.

Selective separation is a phenomenon in which a substance or substances in the separation component preferentially penetrate the membrane layer due to the particularity of the membrane material and the separation component. For instance, as Jin Wanqin et al[55]. studied the separation of water and Dimethyl Carbonate (DMC) mixture by graphene oxide membrane[56, 57], they found that even if DMC and water can pass through the gap of the ink oxide membrane, the water content is only 2% in DMC. The flux of water in the water system is still greater than the flux of DMC, demonstrating that the graphene oxide membrane can be passed through preferentially by water molecules. Yongsoon Shin et al.[58] have studied highly selective supported graphene oxide membranes for water-ethanol separation, which shows excellent water/ethanol at elevated temperatures.

Declarations

Competing interests statement:

The authors declare no competing interests.

References

1. Bracha, D., M.T. Walls, and C.P. Brangwynne, *Probing and engineering liquid-phase organelles*. Nat Biotechnol, 2019. **37**(12): p. 1435–1445.
2. Kopf, M., C. Schneider, and S.P. Nobs, *The development and function of lung-resident macrophages and dendritic cells*. Nat Immunol, 2015. **16**(1): p. 36–44.
3. Fujioka, Y., et al., *Phase separation organizes the site of autophagosome formation*. Nature, 2020. **578**(7794): p. 301–305.
4. Hendriks, K.H., et al., *High-Performance Oligomeric Catholytes for Effective Macromolecular Separation in Nonaqueous Redox Flow Batteries*. ACS Cent Sci, 2018. **4**(2): p. 189–196.
5. Lu, W., et al., *Porous membranes in secondary battery technologies*. Chem Soc Rev, 2017. **46**(8): p. 2199–2236.
6. Uhlenhuth, E., *CULTIVATION OF THE SKIN EPITHELIUM OF THE ADULT FROG, RANA PIPIENS*. J Exp Med, 1914. **20**(6): p. 614–34.
7. Kallithrakas-Kontos, N.G., et al., *Selective Membrane Complexation and Uranium Isotopes Analysis in Tap Water and Seawater Samples*. Anal Chem, 2018. **90**(7): p. 4611–4615.
8. Fujiwara, M. and T. Imura, *Photo Induced Membrane Separation for Water Purification and Desalination Using Azobenzene Modified Anodized Alumina Membranes*. ACS Nano, 2015. **9**(6): p. 5705–12.
9. Wang, X., et al., *Poly(vinylidene Fluoride-Hexafluoropropylene) Porous Membrane with Controllable Structure and Applications in Efficient Oil/Water Separation*. Materials (Basel), 2018. **11**(3).
10. Khulbe, K.C. and T. Matsuura, *Thin Film Composite and/or Thin Film Nanocomposite Hollow Fiber Membrane for Water Treatment, Pervaporation, and Gas/Vapor Separation*. Polymers (Basel), 2018. **10**(10).
11. Qi, B., et al., *Strict molecular sieving over electrodeposited 2D-interspacing-narrowed graphene oxide membranes*. Nat Commun, 2017. **8**(1): p. 825.
12. Huang, K., et al., *Micropatterned Ultrathin MOF Membranes with Enhanced Molecular Sieving Property*. Angew Chem Int Ed Engl, 2018. **57**(42): p. 13892–13896.
13. Han, J.L., et al., *Functional graphene oxide membrane preparation for organics/inorganic salts mixture separation aiming at advanced treatment of refractory wastewater*. Sci Total Environ, 2018. **628-629**: p. 261–270.
14. Labrado, D., et al., *Identification by NMR of key compounds present in beer distillates and residual phases after dealcoholization by vacuum distillation*. J Sci Food Agric, 2020. **100**(10): p. 3971–3978.

15. Deshpande, S.S., et al., *Freeze concentration of fruit juices*. Crit Rev Food Sci Nutr, 1984. **20**(3): p. 173–248.
16. Stein, S., et al., *Redox condition of saline groundwater from coastal aquifers influences reverse osmosis desalination process*. Water Res, 2020. **188**: p. 116508.
17. De Francesco, G., et al., *Effects of Operating Conditions during Low-Alcohol Beer Production by Osmotic Distillation*. J Agric Food Chem, 2014. **62**(14): p. 3279–3286.
18. Braeken, L., B. Van der Bruggen, and C. Vandecasteele, *Regeneration of brewery waste water using nanofiltration*. Water Res, 2004. **38**(13): p. 3075–82.
19. Freger, V., *Swelling and morphology of the skin layer of polyamide composite membranes: an atomic force microscopy study*. Environ Sci Technol, 2004. **38**(11): p. 3168–75.
20. Yao, L., et al., *Effects of fermentation substrate conditions on corn-soy co-fermentation for fuel ethanol production*. Bioresour Technol, 2012. **120**: p. 140–8.
21. Labanda, J., et al., *Membrane separation technology for the reduction of alcoholic degree of a white model wine*. LWT - Food Science and Technology, 2009. **42**(8): p. 1390–1395.
22. Andrés-Iglesias, C., et al., *Simulation and flavor compound analysis of dealcoholized beer via one-step vacuum distillation*. Food Research International, 2015. **76**: p. 751–760.
23. Henriques, P., et al., *Controlled freeze-thawing test to determine the degree of deionization required for tartaric stabilization of wines by electrodialysis*. Food Chem, 2019. **278**: p. 84–91.
24. Martínez-Pérez, M.P., et al., *Evaluating Alternatives to Cold Stabilization in Wineries: The Use of Carboxymethyl Cellulose, Potassium Polyaspartate, Electrodialysis and Ion Exchange Resins*. Foods, 2020. **9**(9).
25. Oberholster, A., L.M. Carstens, and W.J. du Toit, *Investigation of the effect of gelatine, egg albumin and cross-flow microfiltration on the phenolic composition of Pinotage wine.* Food Chem, 2013. **138**(2-3): p. 1275-81.
26. Martínez-Lapuente, L., Z. Guadalupe, and B. Ayestarán, *Effect of egg albumin fining, progressive clarification and cross-flow microfiltration on the polysaccharide and proanthocyanidin composition of red varietal wines*. Food Res Int, 2017. **96**: p. 235–243.
27. Kitani, H., et al., *Dewatering of algal suspension using microfiltration with cross flow in the presence of magnetite as a filter aid*. Biotechnol Prog, 2020. **36**(4): p. e2979.
28. BELLEVILLE, M.-P., et al., *Fouling Colloids During Microporous Alumina Membrane Filtration of Wine*. Journal of Food Science, 1992. **57**(2): p. 396–400.
29. Czekaj, P., F. López, and C. Güell, *Membrane fouling during microfiltration of fermented beverages*. Journal of Membrane Science, 2000. **166**(2): p. 199–212.
30. Vernhet, A., D. Cartalade, and M. Moutounet, *Contribution to the understanding of fouling build-up during microfiltration of wines*. Journal of Membrane Science, 2003. **211**(2): p. 357–370.
31. Ban, T., et al., *Preparation of a Completely Oriented Molecular Sieve Membrane*. Angew Chem Int Ed Engl, 1999. **38**(22): p. 3324–3326.

32. Huang, A., et al., *Molecular-sieve membrane with hydrogen permselectivity: ZIF-22 in LTA topology prepared with 3-aminopropyltriethoxysilane as covalent linker*. Angew Chem Int Ed Engl, 2010. **49**(29): p. 4958–61.
33. Huang, A., et al., *Neutral and cation-free LTA-type aluminophosphate (AlPO(4)) molecular sieve membrane with high hydrogen permselectivity*. J Am Chem Soc, 2010. **132**(7): p. 2140–1.
34. Lew, C.M., R. Cai, and Y. Yan, *Zeolite thin films: from computer chips to space stations*. Acc Chem Res, 2010. **43**(2): p. 210–9.
35. Kayler, Z.E., et al., *Soil evaporation and organic matter turnover in the Sub-Taiga and Forest-Steppe of southwest Siberia*. Sci Rep, 2018. **8**(1): p. 10904.
36. Booij, J.C., et al., *The dynamic nature of Bruch's membrane*. Prog Retin Eye Res, 2010. **29**(1): p. 1–18.
37. Kang, C.C., et al., *Single cell-resolution western blotting*. Nat Protoc, 2016. **11**(8): p. 1508–30.
38. Marmor, M.F., et al., *Recommendations on Screening for Chloroquine and Hydroxychloroquine Retinopathy (2016 Revision)*. Ophthalmology, 2016. **123**(6): p. 1386–94.
39. Chaisaingmongkol, J., et al., *Common Molecular Subtypes Among Asian Hepatocellular Carcinoma and Cholangiocarcinoma*. Cancer Cell, 2017. **32**(1): p. 57-70.e3.
40. Zhao, P., et al., *Characterization of the Key Aroma Compounds in Chinese Syrah Wine by Gas Chromatography-Olfactometry-Mass Spectrometry and Aroma Reconstitution Studies*. Molecules, 2017. **22**(7).
41. Zhu, F., et al., *Applications of in vivo and in vitro solid-phase microextraction techniques in plant analysis: A review*. Anal Chim Acta, 2013. **794**: p. 1–14.
42. Azizi, A. and C.S. Bottaro, *A critical review of molecularly imprinted polymers for the analysis of organic pollutants in environmental water samples*. J Chromatogr A, 2020. **1614**: p. 460603.
43. Kritsunankul, O., B. Pramote, and J. Jakmunee, *Flow injection on-line dialysis coupled to high performance liquid chromatography for the determination of some organic acids in wine*. Talanta, 2009. **79**(4): p. 1042–9.
44. Regmi, U., M. Palma, and C.G. Barroso, *Direct determination of organic acids in wine and wine-derived products by Fourier transform infrared (FT-IR) spectroscopy and chemometric techniques*. Anal Chim Acta, 2012. **732**: p. 137–44.
45. Mortera, P., et al., *Multivariate analysis of organic acids in fermented food from reversed-phase high-performance liquid chromatography data*. Talanta, 2018. **178**: p. 15–23.
46. Fiechter, G., D. Pavelescu, and H.K. Mayer, *UPLC analysis of free amino acids in wines: profiling of on-lees aged wines*. J Chromatogr B Analyt Technol Biomed Life Sci, 2011. **879**(17-18): p. 1361–6.
47. Wang, Y.Q., et al., *Rapid HPLC analysis of amino acids and biogenic amines in wines during fermentation and evaluation of matrix effect*. Food Chem, 2014. **163**: p. 6–15.
48. Wu, N., et al., *Antioxidant activities and xanthine oxidase inhibitory effects of extracts and main polyphenolic compounds obtained from Geranium sibiricum L*. J Agric Food Chem, 2010. **58**(8): p. 4737–43.

49. Mamaghani, A.H., F. Haghighat, and C.S. Lee, *Hydrothermal/solvothermal synthesis and treatment of TiO(2) for photocatalytic degradation of air pollutants: Preparation, characterization, properties, and performance*. Chemosphere, 2019. **219**: p. 804–825.
50. Zargazi, M. and M.H. Entezari, *Sonochemical versus hydrothermal synthesis of bismuth tungstate nanostructures: Photocatalytic, sonocatalytic and sonophotocatalytic activities*. Ultrason Sonochem, 2019. **51**: p. 1–11.
51. Tilley, S.D., A. Selloni, and T. Hisatomi, *Preface to Special Issue of ChemSusChem-Water Splitting: From Theory to Practice*. ChemSusChem, 2019. **12**(9): p. 1771–1774.
52. Dong, R., et al., *Sequence-defined multifunctional polyethers via liquid-phase synthesis with molecular sieving*. Nat Chem, 2019. **11**(2): p. 136–145.
53. Dong, R., et al., *Author Correction: Sequence-defined multifunctional polyethers via liquid-phase synthesis with molecular sieving*. Nat Chem, 2019. **11**(2): p. 184.
54. Ueno, K., et al., *Hydrophobic *BEA-Type Zeolite Membranes on Tubular Silica Supports for Alcohol/Water Separation by Pervaporation*. Membranes (Basel), 2019. **9**(7).
55. Huang, K., et al., *A graphene oxide membrane with highly selective molecular separation of aqueous organic solution*. Angew Chem Int Ed Engl, 2014. **53**(27): p. 6929–32.
56. Protsak, I., et al., *Cleavage of Organosiloxanes with Dimethyl Carbonate: A Mild Approach To Graft-to-Surface Modification*. Langmuir, 2018. **34**(33): p. 9719–9730.
57. Lee, S.J.R., et al., *Projection-Based Wavefunction-in-DFT Embedding*. Acc Chem Res, 2019. **52**(5): p. 1359–1368.
58. Shin, Y., et al., *Highly Selective Supported Graphene Oxide Membranes for Water-Ethanol Separation*. Sci Rep, 2019. **9**(1): p. 2251.

Tables

Table 1 . Change of β when mw = 100

§	mz	β	ma	mb	mq	mc	mw	X
11.50%	100.23	0.148562922	15.23	119.49	111.47	76.98	100	1
11.50%	100.11	0.139357346	14.22	112.45	111.47	84.91	100	2
11.50%	100.02	0.167377295	17.23	110.55	111.47	83.71	100	3
11.50%	99.99	0.133888625	13.65	115.93	111.47	81.88	100	4
11.50%	100.14	0.142377878	14.54	112.01	111.47	85.06	100	5
11.50%	100.64	0.13512061	13.78	116.35	111.47	81.98	100	6
11.50%	100.21	0.140220622	14.32	115.17	111.47	82.19	100	7
11.50%	100.11	0.139646047	14.25	112.22	111.47	85.11	100	8
11.50%	100.03	0.151455308	15.54	118.78	111.47	77.18	100	9

Table 2 . Change of β when mw = 200

§	mz	β	ma	mb	mq	mc	mw	X
11.50%	100.25	0.072362119	14.63	113.43	111.47	83.66	200	1
11.50%	100.24	0.073188133	14.80	112.98	111.47	83.93	200	2
11.50%	100.80	0.072317032	14.62	113.56	111.47	84.09	200	3
11.50%	100.41	0.071148296	14.38	114.02	111.47	83.48	200	4
11.50%	99.56	0.069982739	14.14	113.49	111.47	83.4	200	5
11.50%	99.34	0.073476146	14.86	112.34	111.47	83.61	200	6
11.50%	100.17	0.074012897	14.97	112.57	111.47	84.1	200	7
11.50%	100.85	0.072803845	14.72	113.25	111.47	84.35	200	8
11.50%	100.69	0.069643913	14.07	114.53	111.47	83.56	200	9

Table 3 . Change of β when mw = 400

§	mz	β	ma	mb	mq	mc	mw	X
11.50%	100.47	0.035934927	14.45	113.25	111.47	84.24	400	1
11.50%	100.08	0.035267852	14.18	114.22	111.47	83.15	400	2
11.50%	100.84	0.035147021	14.13	113.74	111.47	84.44	400	3
11.50%	100	0.037066031	14.91	112.89	111.47	83.67	400	4
11.50%	100.59	0.036180242	14.55	113.74	111.47	83.77	400	5
11.50%	100.23	0.034873766	14.02	114.46	111.47	83.22	400	6
11.50%	100.36	0.036254514	14.58	113.27	111.47	83.98	400	7
11.50%	100.83	0.0353439	14.21	113.78	111.47	84.31	400	8
11.50%	100.86	0.034998201	14.07	114.36	111.47	83.9	400	9

Table 4 . Change of β when mw = 800

§	mz	β	ma	mb	mq	mc	mw	X
11.50%	100.36	0.017791412	14.27	113.57	111.47	83.99	800	1
11.50%	100.5	0.017642744	14.15	113.31	111.47	84.51	800	2
11.50%	100.28	0.018336875	14.71	113.78	111.47	83.26	800	3
11.50%	100.78	0.018163523	14.57	113.84	111.47	83.84	800	4
11.50%	100.89	0.018250571	14.64	113.44	111.47	84.28	800	5
11.50%	100.65	0.018585269	14.91	113.24	111.47	83.97	800	6
11.50%	100.87	0.01782863	14.30	114.06	111.47	83.98	800	7
11.50%	100.13	0.01789038	14.35	113.87	111.47	83.38	800	8
11.50%	100.02	0.017530904	14.06	113.25	111.47	84.18	800	9
11.50%	100.71	0.018324606	14.7	113.96	111.47	83.52	800	10
11.50%	100.54	0.018027137	14.46	113.57	111.47	83.98	800	11
11.50%	100.59	0.017493358	14.03	114.55	111.47	83.48	800	12

Table 5.Calculate alcohol by formula and Alcohol accuracy measured by machine

Sample	Calculate alcohol by formula	Alcohol accuracy measured by machine	Data Error
1	0.140220622	0.139760979	0.996722
2	0.073188133	0.07283986	0.9952414
3	0.073476146	0.072938183	0.9926784
4	0.037066031	0.036907435	0.995721272
5	0.036254514	0.035947935	0.9915437
6	0.034998201	0.032342583	0.9241213
7	0.018163523	0.018013493	0.99174
8	0.018585269	0.018481192	0.9944
9	0.018324606	0.018205533	0.993502

Table.6 Table of test data before and after organic acid content of three samples

Content of organic acids in wine (g / L)						
Sample	Sample1		Sample2		Sample3	
Components	Before	After	Before	After	Before	After
Tartaric acid	3.128	3.105	3.438	3.349	3.265	3.169
Malic acid	0.238	0.226	0.246	0.217	0.287	0.267
Succinic acid	1.211	1.196	2.978	2.792	2.35	2.165
Malonic acid	0.518	0.501	0.411	0.358	0.556	0.459
Lactic acid	2.536	2.435	1.962	1.823	2.282	2.158
Quinic acid	0.322	0.311	0.328	0.286	0.343	0.316
Citric acid	0.318	0.294	0.119	0.094	0.24	0.164
Acetic acid	0.327	0.301	0.146	0.135	0.045	0.041
Vc	trace	trace	trace	trace	trace	trace
Fumaric acid	trace	trace	trace	trace	trace	trace
Total acid	8.596	8.369	9.628	9.054	9.368	8.739

Table.7 Comparison of amino acids before and after filtration

Types of amino acids	content/（μmol·L-1）					
	Sample1		Sample2		Sample3	
	Before	After	Before	After	Before	After
Gly	37.6523	37.0782	37.2758	36.5174	34.5102	33.9016
Ala	37.6529	37.2284	36.8999	36.1421	34.5104	33.9006
Val	84.4522	83.4035	81.9186	80.2445	80.5973	79.2099
Leu	98.7430	97.6152	90.8435	88.9690	92.2467	90.6588
Ile	43.1802	42.6562	39.7257	38.9131	40.8211	40.1037
Phe	59.5268	58.4946	55.9552	54.8167	56.2734	55.3048
Trp	0.0000	0.0000	0.0000	0.0000	0.0000	0.0000
Tyr	0.0000	0.0000	0.0000	0.0000	0.0000	0.0000
Asp	66.6419	65.4862	61.0773	59.8397	63.0002	61.9158
Asn	66.6585	65.4977	65.7612	64.4248	63.0141	61.9294
Glu	201.6585	198.0568	187.9659	184.1652	192.4476	189.0967
Lys	81.6542	80.7368	76.1152	78.0000	77.1914	75.8680
Gln	51.6548	50.8674	47.6077	46.6454	50.5524	49.6822
Met	61.6472	60.5713	57.4647	56.3033	60.0772	59.0430
Ser	94.5448	93.0877	91.8626	90.0057	92.2115	90.5905
Thr	62.4987	61.5458	60.8238	59.5944	59.2194	58.2002
Cys	98.6542	97.2210	96.8158	94.8590	94.1879	92.5665
Pro	65988.5870	65022.7549	60813.7620	59549.5844	63001.1409	61914.8996
His	71.6549	70.7870	68.4173	67.0117	66.4852	65.3408
Arg	438.2138	432.8973	401.6412	393.3874	406.6082	399.6091

Figures

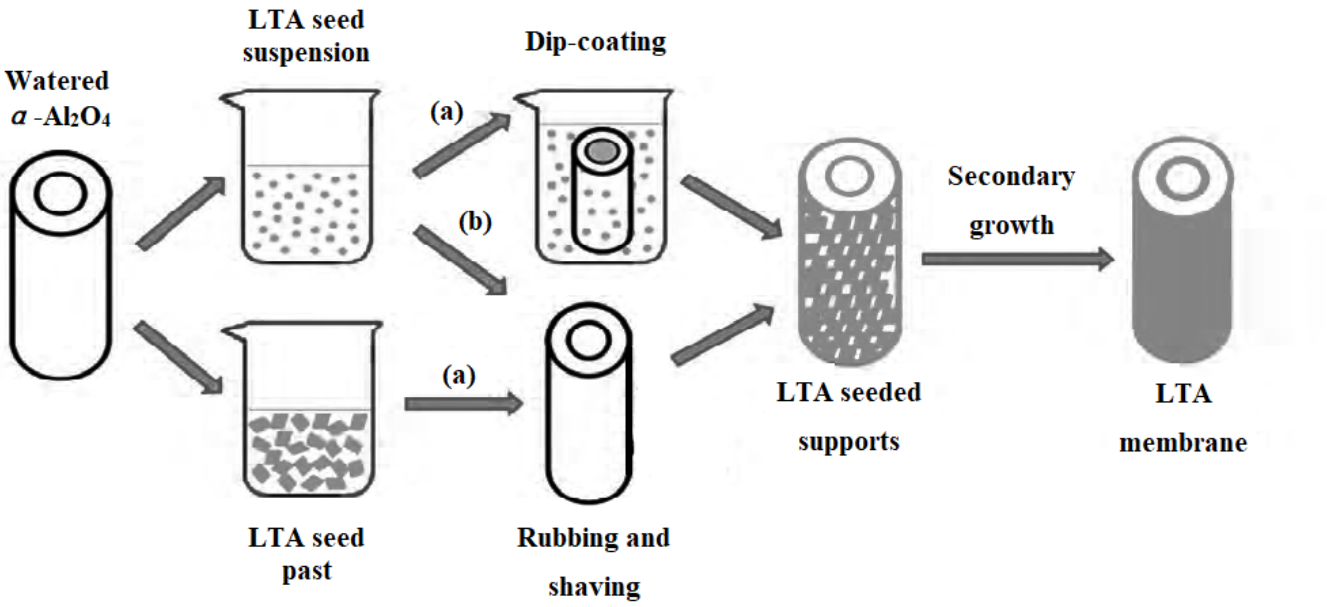

Figure 1

Process for the fabrication of continuous and compact LTA membrane on α-Al2O3 tube

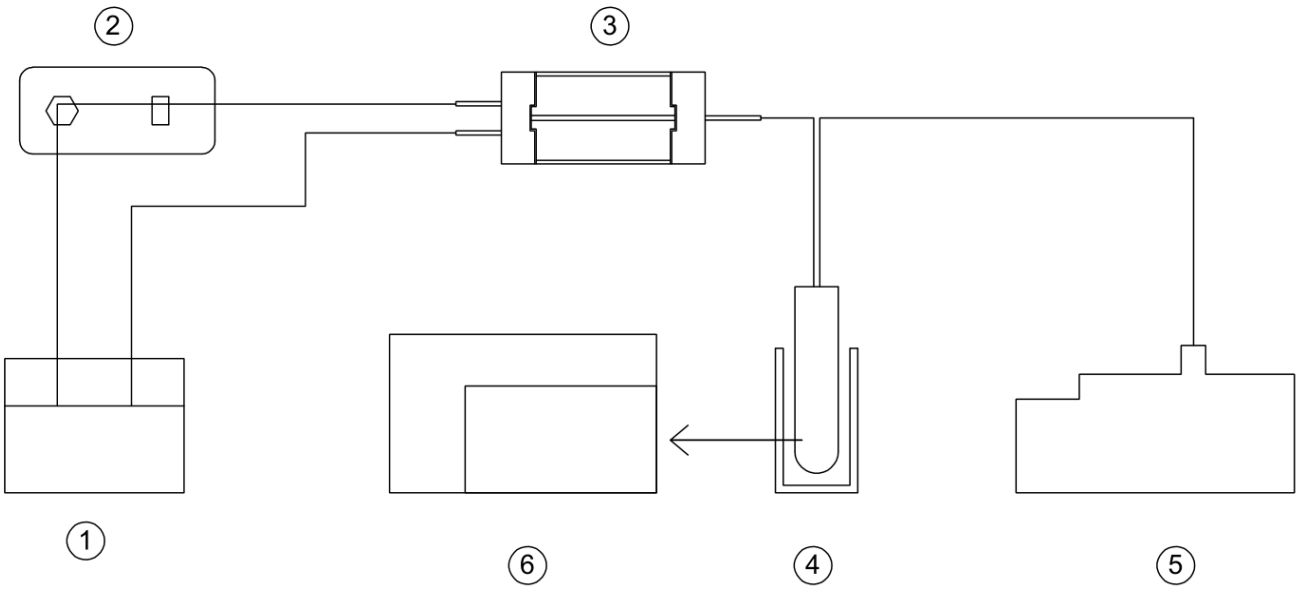

Figure 2

Schematic diagram of LTA membrane separation unit

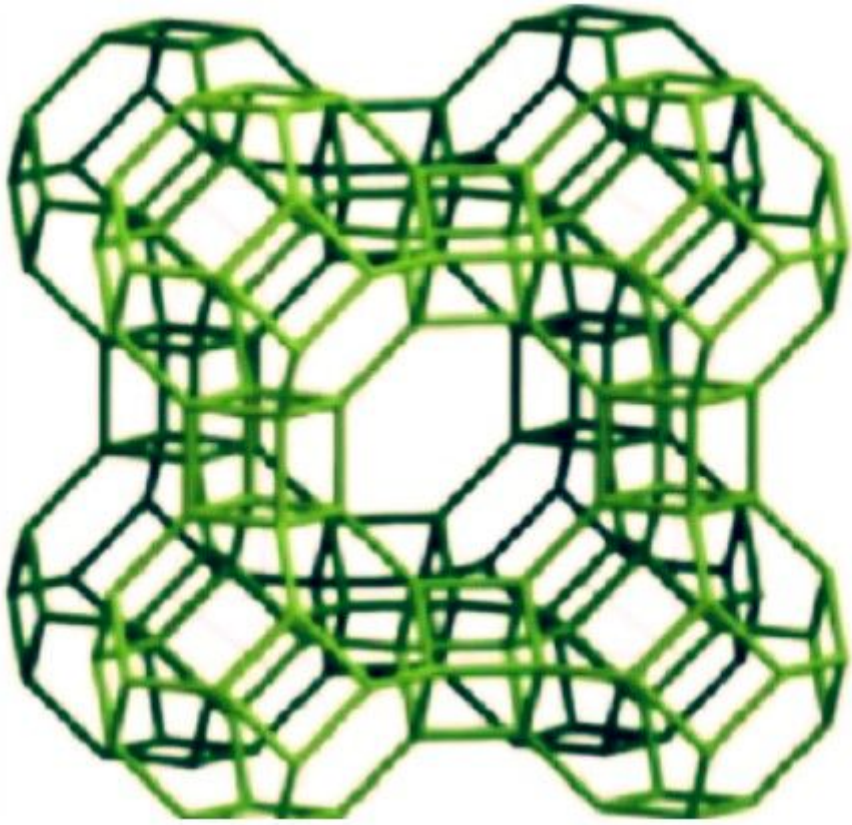

Figure 3

The LTA vertical channel structure

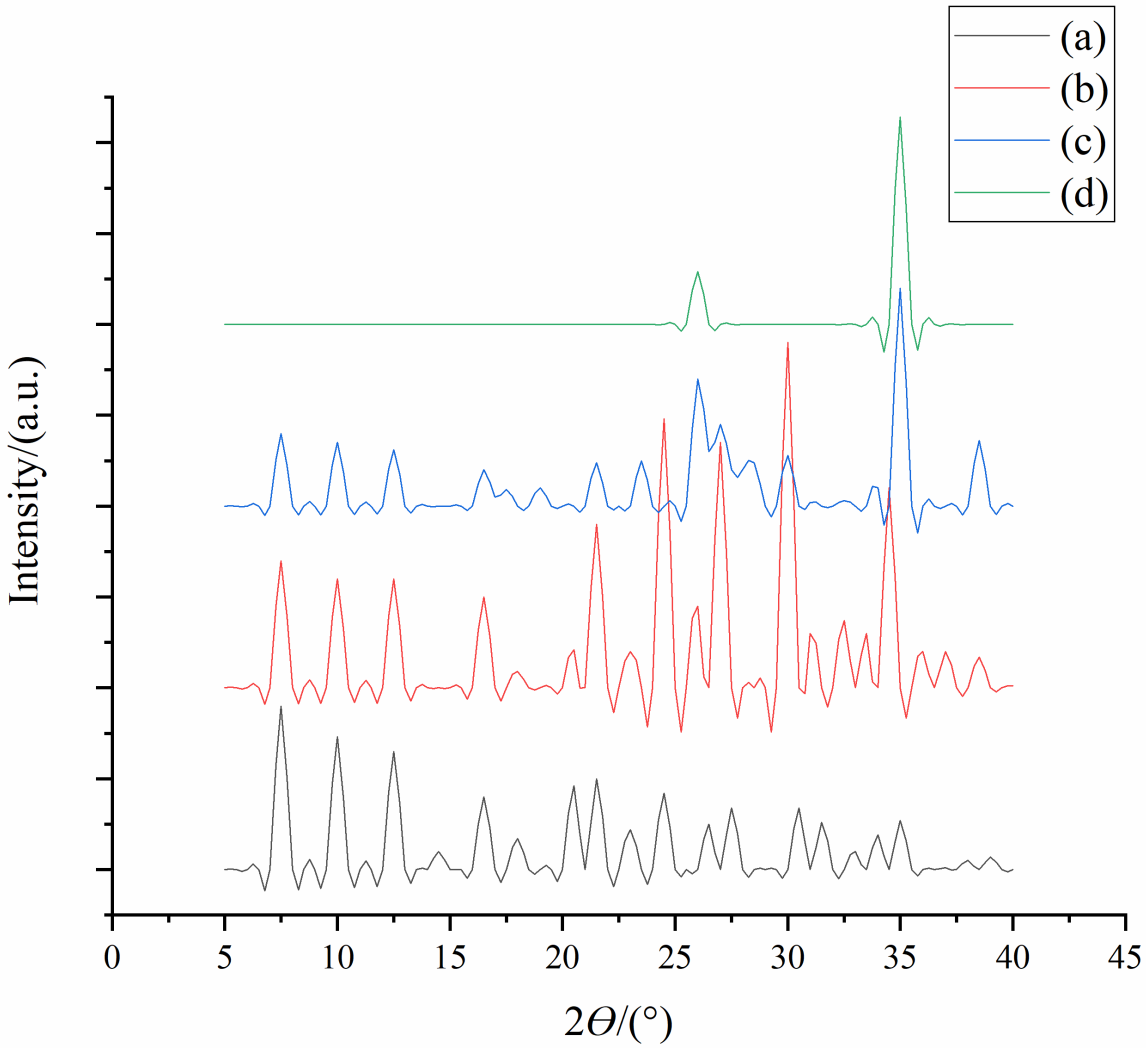

Figure 4

XRD patterns of (a) simulated LTA structure; (b) LTA power; (c) LTA membrane and (d) substation tube

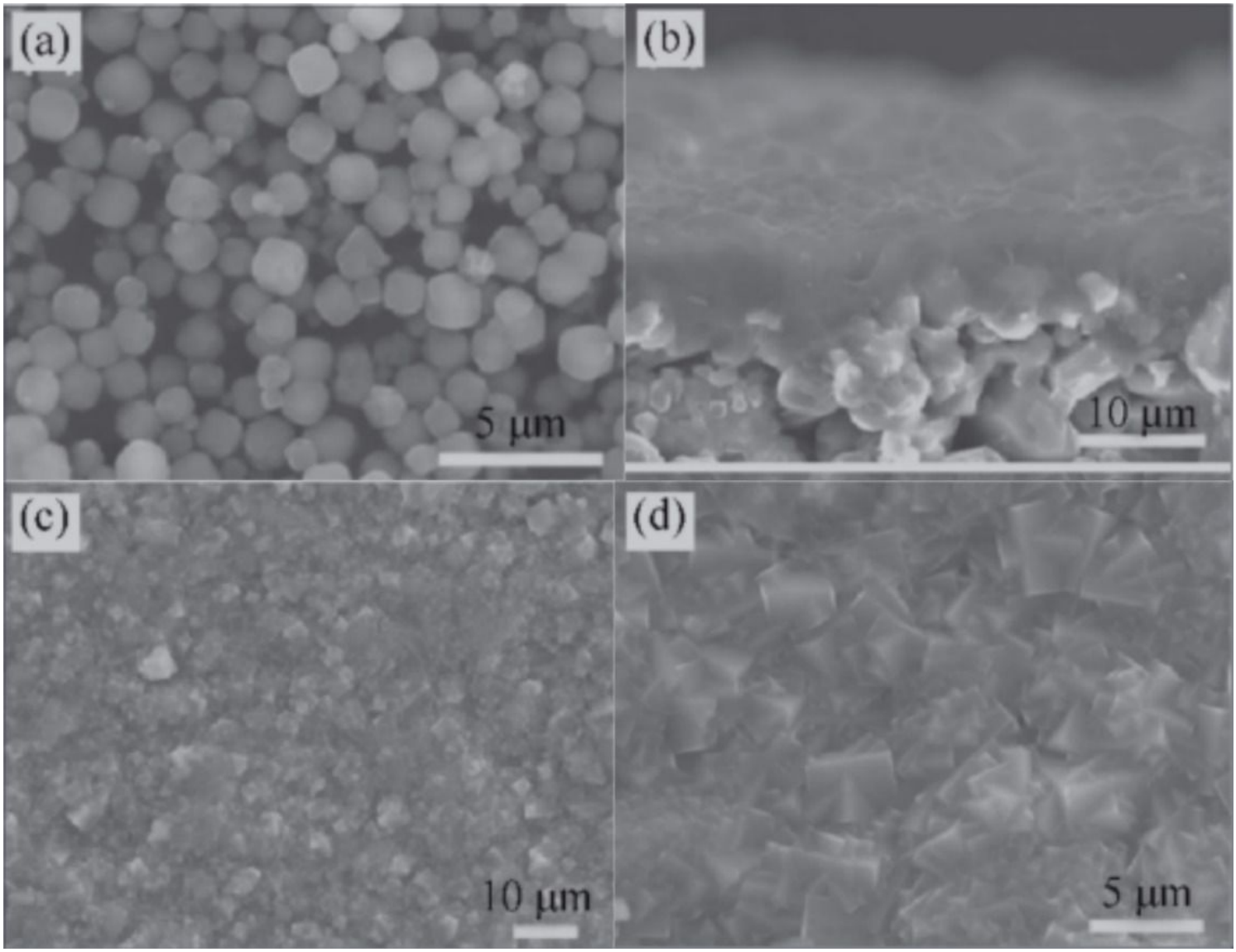

Figure 5

a SEM picture of (a) LTA power; (b) cross section of LTA membrane; (c) and (d) top view of LTA membrane of different magnification

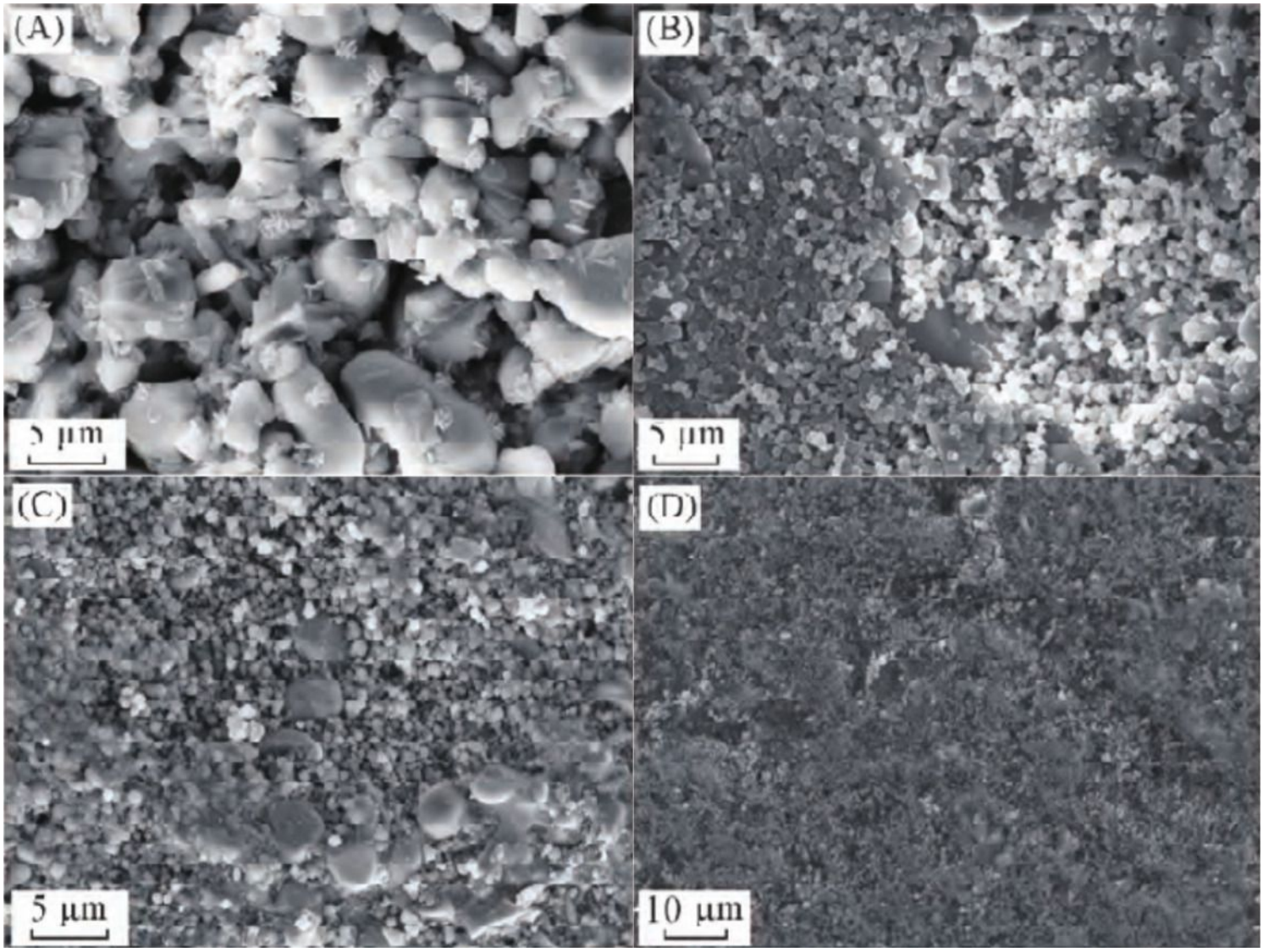

Figure 6

SEM images of α-Al2O3 (A) and seeded support by dip-coating seed suspension (B), rubbing seed suspension with shaving (C) and rubbing seed past with shaving (D)

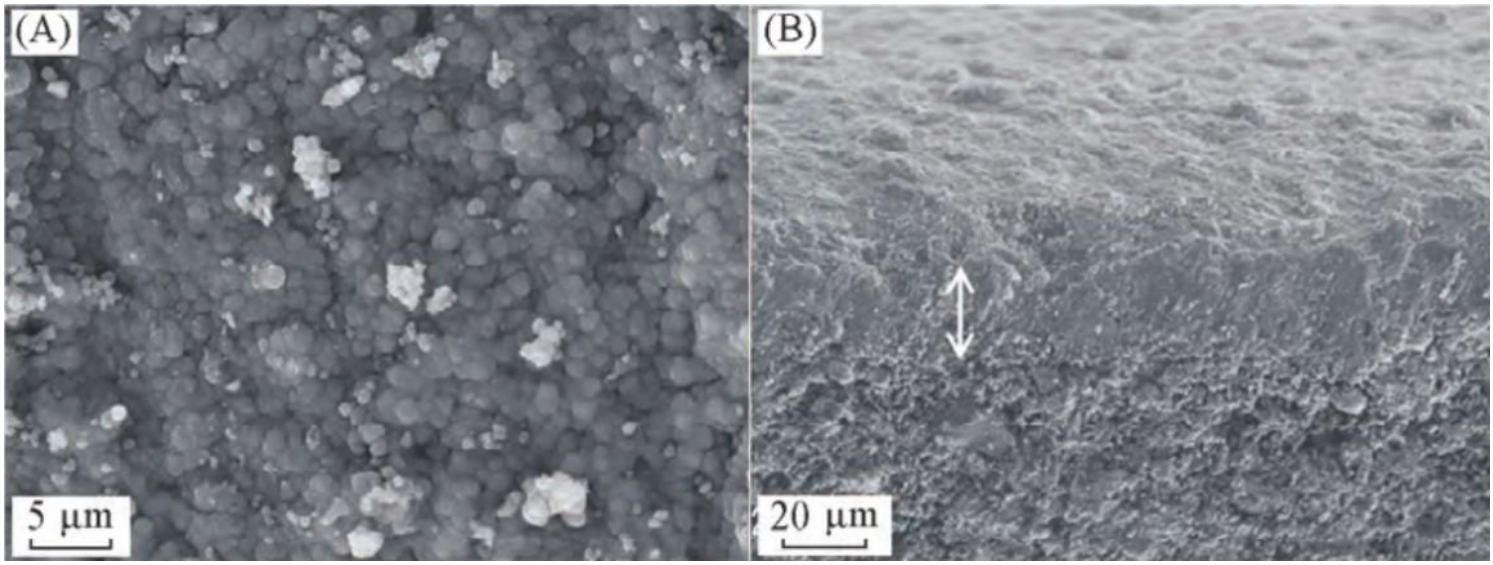

Figure 7

SEM images of zeolite membranes after filtering from the top view (A) and cross section view (B)

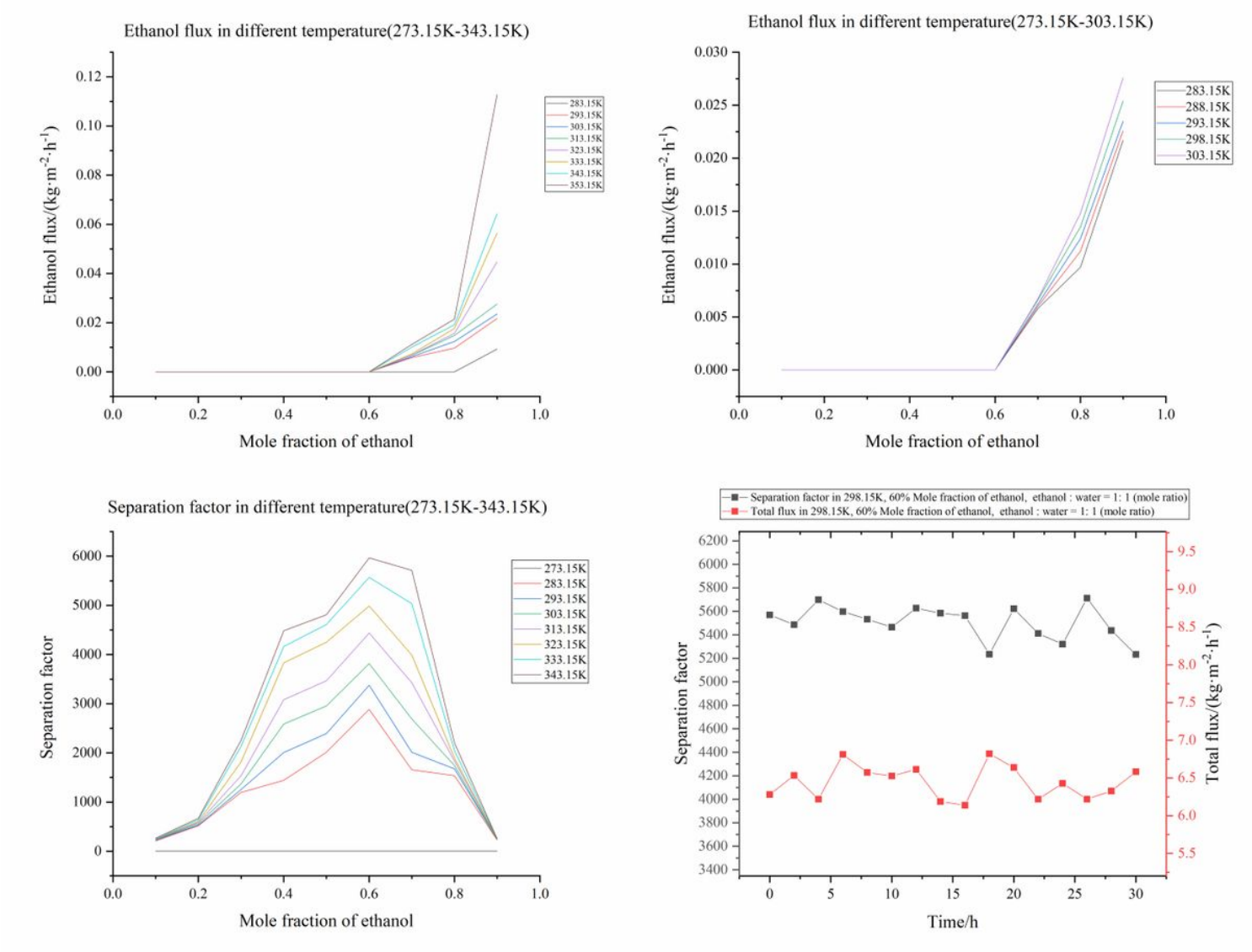

Figure 8

The curves obtained versus mole fractions of ethanol at 25°C (a) flux of ethanol, (b) flux of water and (c) separation factor; (d) curves of total flux and separation factor versus time

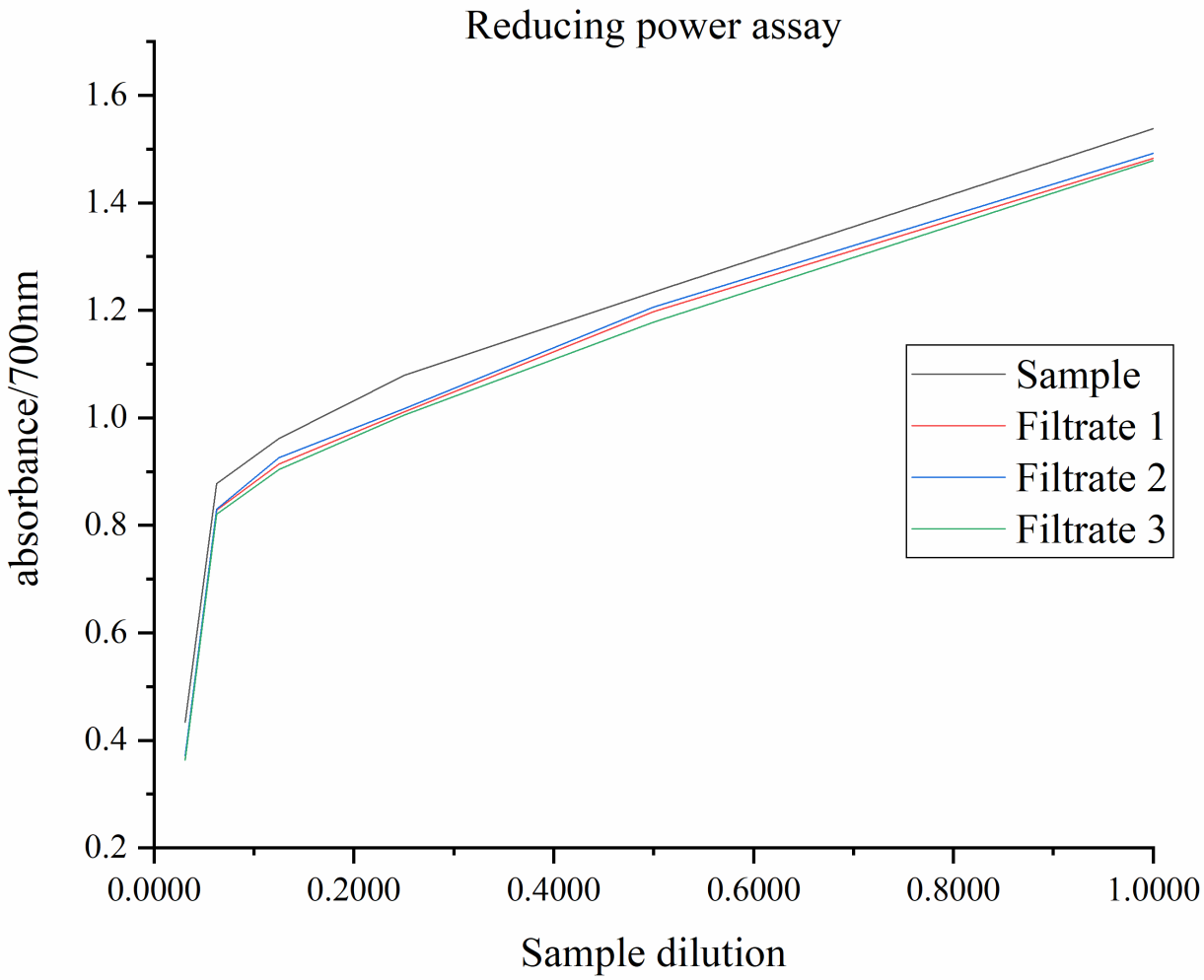

Figure 9

Reducing power assay, The Before is the curve measured by unfiltered sample, The After 1 is the curve measured by filtered sample 1, The After 2 is the curve measured by filtered sample 2, The Aft